

# Time Domain Multiconductor Transmission Line Analysis Using Effective Internal Impedance

Sangwoo Kim and Dean P. Neikirk\*

Department of Electrical and Computer Engineering  
The University of Texas at Austin  
Austin, Texas 78712  
Tel: (512) 471-4669; Fax: (512) 471-5445  
\*e-mail: neikirk@mail.utexas.edu

## Abstract

A compact skin effect circuit model is used to formulate a time domain boundary condition for lossy transmission lines. The resulting lossless-like multiconductor equations can be used in various time domain calculations, including FDTD.

## Introduction

In the frequency domain, surface impedance boundary conditions (SIBCs) have been used effectively to remove conductors from the solution space, thereby gaining computational speed. In the time domain, Tesche [1] has formulated a convolution-based time-domain integral equation that uses a transformation of frequency domain surface impedance into the time domain. Recently, attempts have been made to overcome these difficulties using Prony's method [2, 3] or Chebyshev approximation [4], which allows the transformation of frequency domain surface impedance into time domain exponentials. However, these procedures can be computationally arduous and the applications have been primarily limited to radiation problems where high frequency approximations (i.e., the surface impedance is a purely local quantity and equal to  $1/\sigma\delta$ ) are sufficient for accurate results. A new effective internal impedance (EII) that gives accurate frequency domain results from DC to very high frequency has also been demonstrated [5]. Here we show how this model can be transformed into a very efficient time domain boundary condition for finite conductivity conductors.

## Circuit Representation

In [5] the EII was used as a boundary condition to accelerate the volume filament method [6]. In this surface ribbon method (SRM), the EII is approximated using the surface impedance of an isolated conductor. Figure 1(a) shows how EII approximations for a rectangular conductor are calculated [7]. The EII of the half plate (Fig. 1a, **A**) is approximated using:

$$Z_A = \sqrt{\frac{j\omega\mu_o}{\sigma}} / W \tanh\left(\sqrt{j\omega\mu_o\sigma} \frac{T}{2}\right), \quad (1)$$

where  $W$  is the width of the ribbon and  $T$  is the thickness of the conductor. The EII of each triangle (Fig. 1a, **B**) is approximated using:

$$Z_B = \frac{\sqrt{-j\omega\mu_o\sigma} J_0(\sqrt{-j\omega\mu_o\sigma} H)}{\sigma W \cdot J_1(\sqrt{-j\omega\mu_o\sigma} H)}, \quad (2)$$

where  $W$  is the base and  $H$  is the height of the iso-triangle.

For time domain calculation it would be advantageous to replace the frequency dependent equations for the EII approximations (eqs. 1 and 2) with frequency independent circuit models. In [8] a compact circuit model consisting of four resistors and three inductors (Fig. 1(b)) was used to accurately model the skin effect in circular conductors. The values of each element are related by the simple rules

$$\frac{R_i}{R_{i+1}} = RR \quad , \quad i = 1, 2, 3. \quad \frac{L_i}{L_{i+1}} = LL \quad , \quad i = 1, 2 \quad , \quad (3)$$

where  $RR$  and  $LL$  are constants to be determined. Requiring the dc resistance and inductance of this circuit model to equal the value from eqs. 1 and 2 yields

$$RR^3 + RR^2 + RR + (1 - \alpha_R) = 0, \quad \text{with } \alpha_R = C_1 \frac{p}{\delta_{\max}} = \frac{R_1}{R_{dc}}, \quad \delta_{\max} = \sqrt{\frac{2}{\omega_{\max} \mu_o \sigma}} \quad (4)$$

$$\left(\frac{1}{LL}\right)^2 + \left(1 + \frac{1}{RR}\right)^2 \frac{1}{LL} + \left(\left[\frac{1}{RR}\right]^2 + \frac{1}{RR} + 1\right)^2 - \alpha_L \left(\left[1 + \frac{1}{RR}\right] \left[\left\{\frac{1}{RR}\right\}^2 + 1\right]\right)^2 = 0 \quad , \quad (5)$$

where  $\alpha_L = C_2 \alpha_R = L_{dc}/L_1$  ,  $\omega_{\max}$  is highest frequency of interest in the input waveform, and  $p$  is the conductor depth parameter, e.g., the height of the iso-triangle, thickness of half plate  $T/2$ , or radius of a circle (for circular conductors).  $C_1$  and  $C_2$  are constants unique to the geometry of the conductor: (0.56, 0.315) for the iso-triangle; (10.8, 0.2) for the half plate; and (0.53, 0.315) for a circular conductor.

Using eqs. 3-5, the values of the circuit model can be determined for a given geometry conductor. In the s-domain, this model can be represented as

$$Z(s) = R_1 \frac{s^3 + a_2 s^2 + a_1 s + a_0}{s^3 + b_2 s^2 + b_1 s + b_0} \quad , \quad (6)$$

where eq. 6 is easily convertible to time domain exponential form. Figure 2 shows the accuracy of this model for a half plate. The accuracy for other geometries is presented in [8].

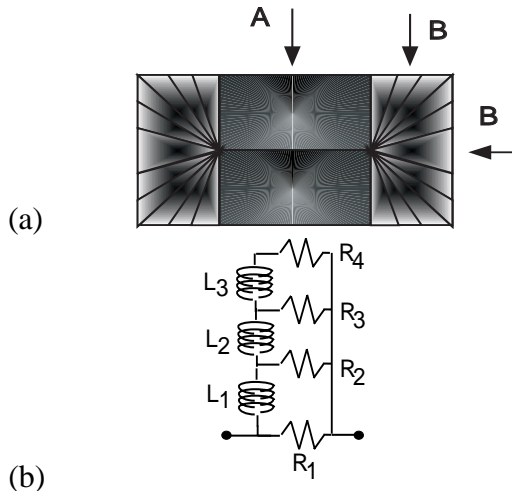


Figure 1: (a) EII calculation of rectangular conductor;  
(b) Compact equivalent circuit model for the EII.

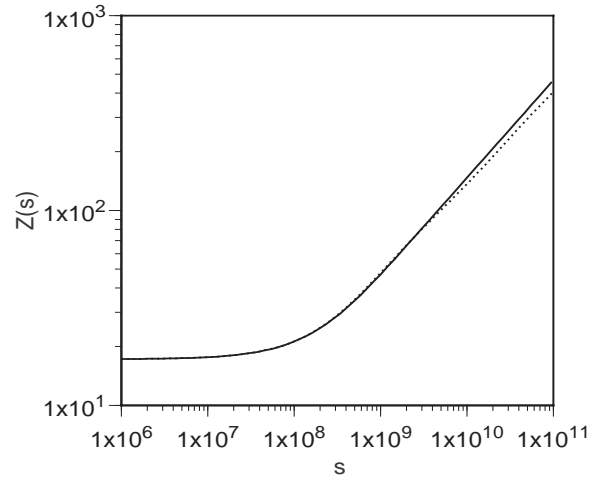


Figure 2) Surface impedance comparison in s-domain. solid line: eq. 1, dotted line: circuit representation.  $W=100 \mu\text{m}$ ,  $T=20 \mu\text{m}$ .

### Formulation of Multiconductor Transmission Line Equation

To formulate a transmission line equation, first one of the ribbons on the return conductor (ground conductor) is considered as a “ground ribbon” (labeled as the 0<sup>th</sup> ribbon) and all the other ribbons are considered as signal ribbons. In the 2-dimensional frequency domain, the equation can be formulated as [5, 6]

$$[Z_{eii}][I] + j\omega[L][I] = \frac{\partial}{\partial z}[V] \quad (7)$$

Equation 7 is formulated under the assumption that all the currents are returned through the 0<sup>th</sup> ribbon, and can be represented in the s-domain as

$$\frac{\partial}{\partial z}[V(s)] = [Z_{eii}(s)][I(s)] + s[L][I(s)] = \left[ \frac{Z_{eii}}{s} \right] s[I(s)] + [L]s[I(s)] \quad (8)$$

Equation 8 can be transformed into the time domain as

$$\frac{\partial}{\partial z}[V(t)] = [\zeta(t)] * \frac{\partial}{\partial t}[I(t)] + [L] \frac{\partial}{\partial t}[I(t)] \quad (9)$$

where  $[\zeta(t)]$  is inverse Laplace transform of  $\left[ \frac{Z_{eii}}{s} \right]$  (which is a rational function) and ‘\*’ is convolution. Using the circuit representation for the EII’s given above  $[\zeta(t)]$  can be easily converted into a sum of exponentials. In [2], the convolution is solved with an approximate recursive relationship

$$Y(n\Delta t) = X(n\Delta t) * (K \cdot e^{Pn\Delta t}) = K\Delta t + e^{P\Delta t} Y((n-1)\Delta t) \quad (10)$$

Applying eq. 10 to eq. 9 results in

$$\frac{\partial}{\partial z}[V(t)] = [[L] + [K]] \frac{\partial}{\partial t}[I(t)] + [V_{ds}(t)] = [L'] \frac{\partial}{\partial t}[I(t)] + [V_{ds}(t)] \quad (11)$$

where  $[V_{ds}(t)]$  is a dependent voltage source (per unit length) that depends on the poles of the EIIs and current values at the previous time, and  $[L']$  is a matrix that depends on the residues of the EIIs and loop inductances of the ribbons. Note that  $[L']$  is time independent, and so eq. 11 is very similar to the equation that results for a lossless transmission line. Another equation can be derived using Kirchoff’s current law,

$$\frac{\partial}{\partial z}[I(t)] = [G][V(t)] + [C] \frac{\partial}{\partial t}[V(t)] \quad (12)$$

To verify the equations given here, an FDTD method [9] is applied to eqs. 11 and 12; this does require the inversion of  $[L']$ , but since  $[L']$  is time independent, the inverse need be calculated only once. As an example problem Fig. 3 shows the cross section of two, coupled, finite thickness microstrip lines over a finite width ground plane. All conductors (including the ground plane) have finite conductivity. Figure 4 compares the FDTD time domain calculation and FFT results using both the full dispersion curve and a simple  $R_{dc}$ -L-C transmission line model. Table 1 compares the computation times required for various methods.

## Conclusions

New time domain multiconductor transmission line equations including frequency dependent skin effect and proximity effect have been derived. Due to the simplicity of the resulting equations, various pre-existing simulation techniques can be easily applied. FDTD result shows good agreement with FFT result, with substantially faster computation compared to even very efficient frequency domain calculations.

This work was sponsored by the DARPA under grant number AFOSR F49620-96-1-0032.

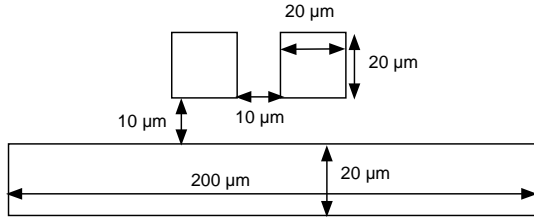


Figure 3: Cross section of coupled microstrip lines used as a test.

method	pre-calculation	main calculation (FDTD or FFT)
SRM-FDTD	0.5 sec	89.5 sec
SRM-FFT	149 sec	0.5 sec
FM-FFT	163,095 sec	0.5 sec

Table 1: Computation time comparison (Sparc 20 workstation). SRM-FDTD: method used in this paper; SRM-FFT: Surface ribbon method [5] in frequency domain, then FFT applied; FM-FFT: Filament method [6, 10] in frequency domain, then FFT applied.

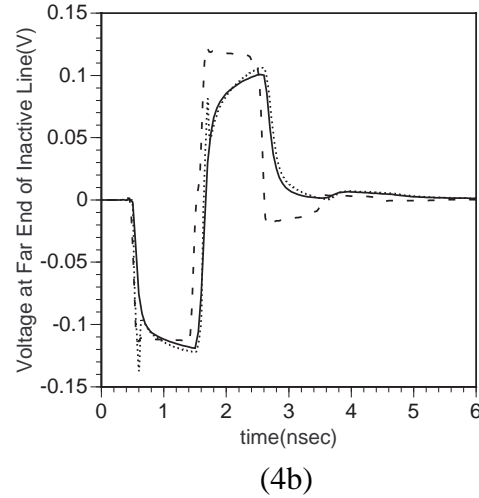
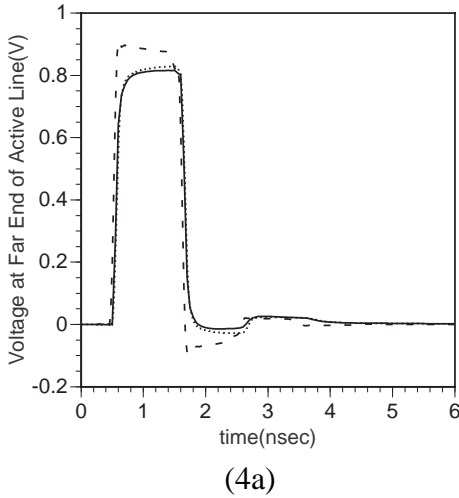


Figure 4: Results for coupled microstrips over a finite ground plane (fig. 3); source resistance used was  $5 \Omega$ , termination resistance  $50 \Omega$ , line lengths 10 cm. (a) Far end response of the active line. (b) Far end response of the quiet (victim) line. Solid line: FFT result; dotted line: FDTD technique in this paper; dashed line:  $R_{dc}$ -L-C circuit.

## References

1. F. M. Tesche, "On the Inclusion of Loss in Time-Domain Solutions of Electromagnetic Interaction Problems," *IEEE Trans. on Electromagnetic Compatibility*, vol. 32, pp. 1-4, 1990.
2. S. Kellali and B. Jecko, "Implementation of a Surface Impedance Formalism at Oblique Incidence in FDTD Method," *IEEE Trans. on Electromagnetic Compatibility*, vol. 35, pp. 347-355, 1993.
3. J. G. Maloney and G. S. Smith, "The Use of Surface Impedance Concepts in the Finite-Difference Time-Domain Method," *IEEE Trans. on Antennas and Propagation*, vol. 40, pp. 38-48, 1992.
4. K. S. Oh and J. E. Schutt-Aine, "An Efficient Implementation of Surface Impedance Boundary Conditions for the Finite-Difference Time-Domain Method," *IEEE Trans. on Antennas and Propagation*, vol. 43, pp. 660-666, 1995.
5. E. Tuncer, B.-T. Lee, and D. P. Neikirk, "Interconnect Series Impedance Determination Using a Surface Ribbon Method," *IEEE 3rd Topical Meeting on Electrical Performance of Electronic Packaging*, Monterey, CA, 1994, pp. 249-252.
6. W. T. Weeks, L. L. Wu, M. F. McAllister, and A. Singh, "Resistive and Inductive Skin Effect in Rectangular Conductors," *IBM Journal of Research Development*, vol. 23, pp. 652-660, 1979.
7. E. Tuncer and D. P. Neikirk, "Efficient Calculation of Surface Impedance for Rectangular Conductors," *Electronics Letters*, vol. 29, pp. 2127-2128, 1993.
8. S. Kim and D. P. Neikirk, "Compact Equivalent Circuit Model for the Skin Effect," *IEEE International Microwave Symposium*, San Francisco, CA, 1996, pp. 1815-1818.
9. C. R. Paul, "Incorporation of Terminal Constraints in the FDTD Analysis of Transmission Lines," *IEEE Trans. on Electromagnetic Compatibility*, vol. 36, pp. 85-91, 1994.
10. M. Kamon, M. J. Tsuk, and J. White, "FASTHENRY: A Multipole-Accelerated 3-D Inductance Extraction Program," *IEEE Transactions on Microwave Theory and Techniques*, vol. 42, pp. 1750-1758, 1994.